

Supporting Information

Nanofibers of Polyaniline and Cu(II)-L-Aspartic Acid for Room-Temperature Carbon Monoxide Gas Sensor

S. F. Nami-Ana ^a, Sh. Nasresfahani ^b, J. Tashkhourian ^{a,*}, M. Shamsipur^c, Z. Zargarpour ^d,
M.H. Sheikhi^d

^a*Department of Chemistry, College of Sciences, Shiraz University, Shiraz 71456, Iran.*

^b*Department of Electrical and Computer Engineering, Golpayegan College of Engineering, Isfahan University of Technology, Golpayegan 87717-67498, Iran.*

^c*Department of Chemistry, Razi University, Kermanshah, Iran.*

^d*School of Electrical and Computer Engineering, Shiraz University, Shiraz, Iran.*

*Corresponding author: Tel: +98 713-6137141

E-mail address: tashkhourian@shirazu.ac.ir (J. Tashkhourian)

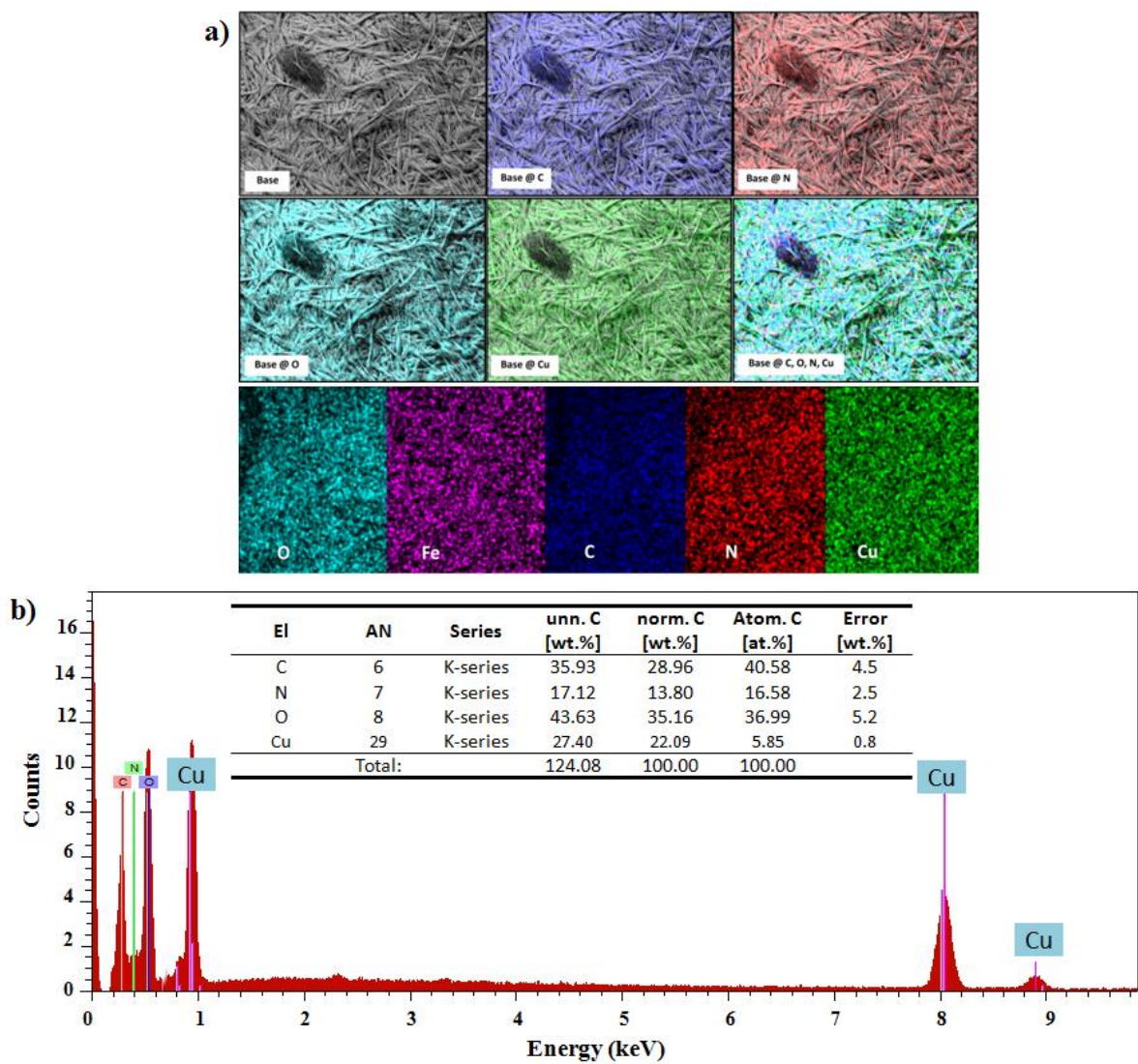


Figure S1. a) The elemental mappings and b) EDX analysis of Cu(II)-L-aspartic acid nanofibers.

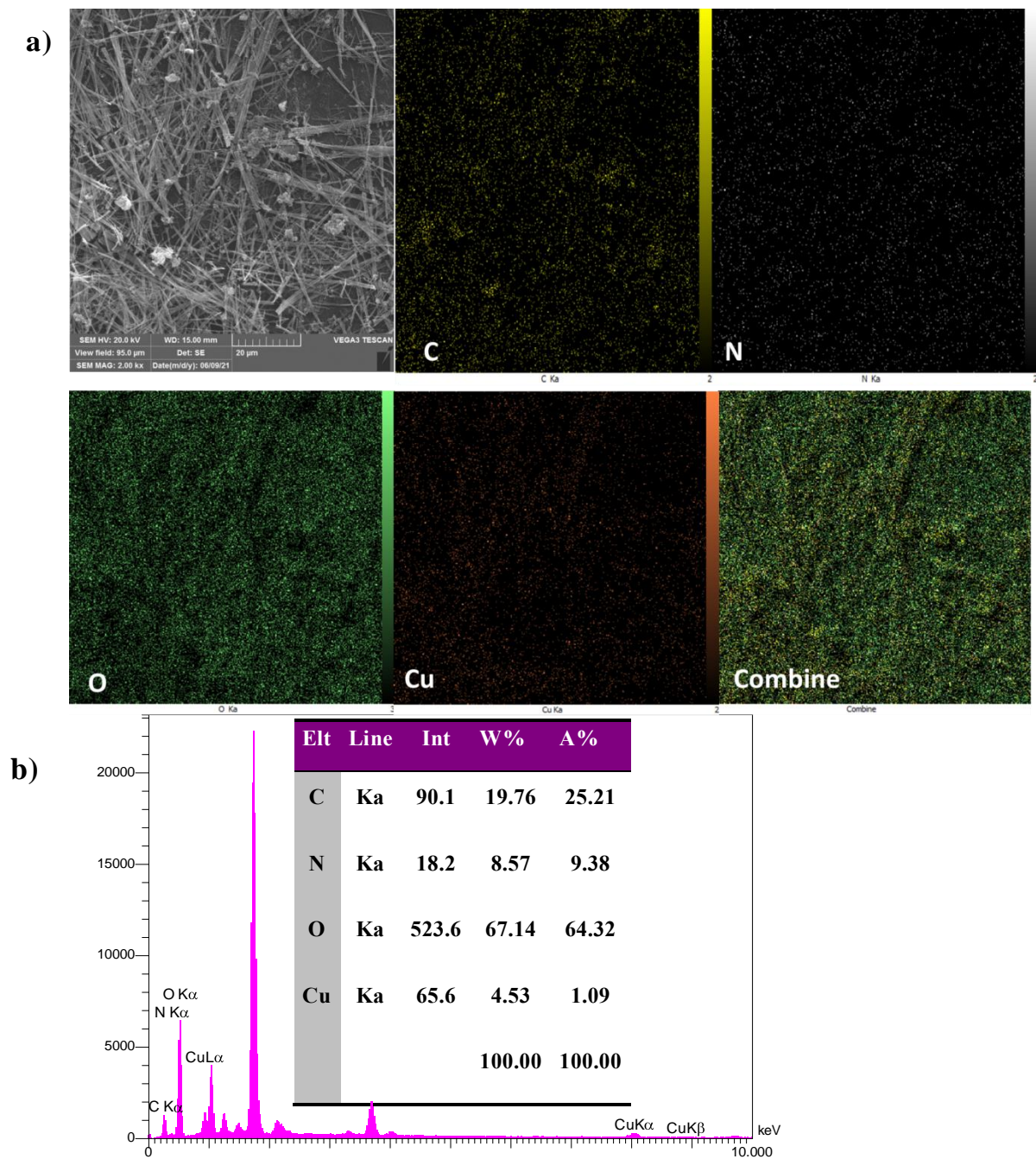


Figure S2. a) The elemental mappings and b) EDX analysis of Cu(II)-L-aspartic acid/ PANI nanofibers composite concentrated solution.

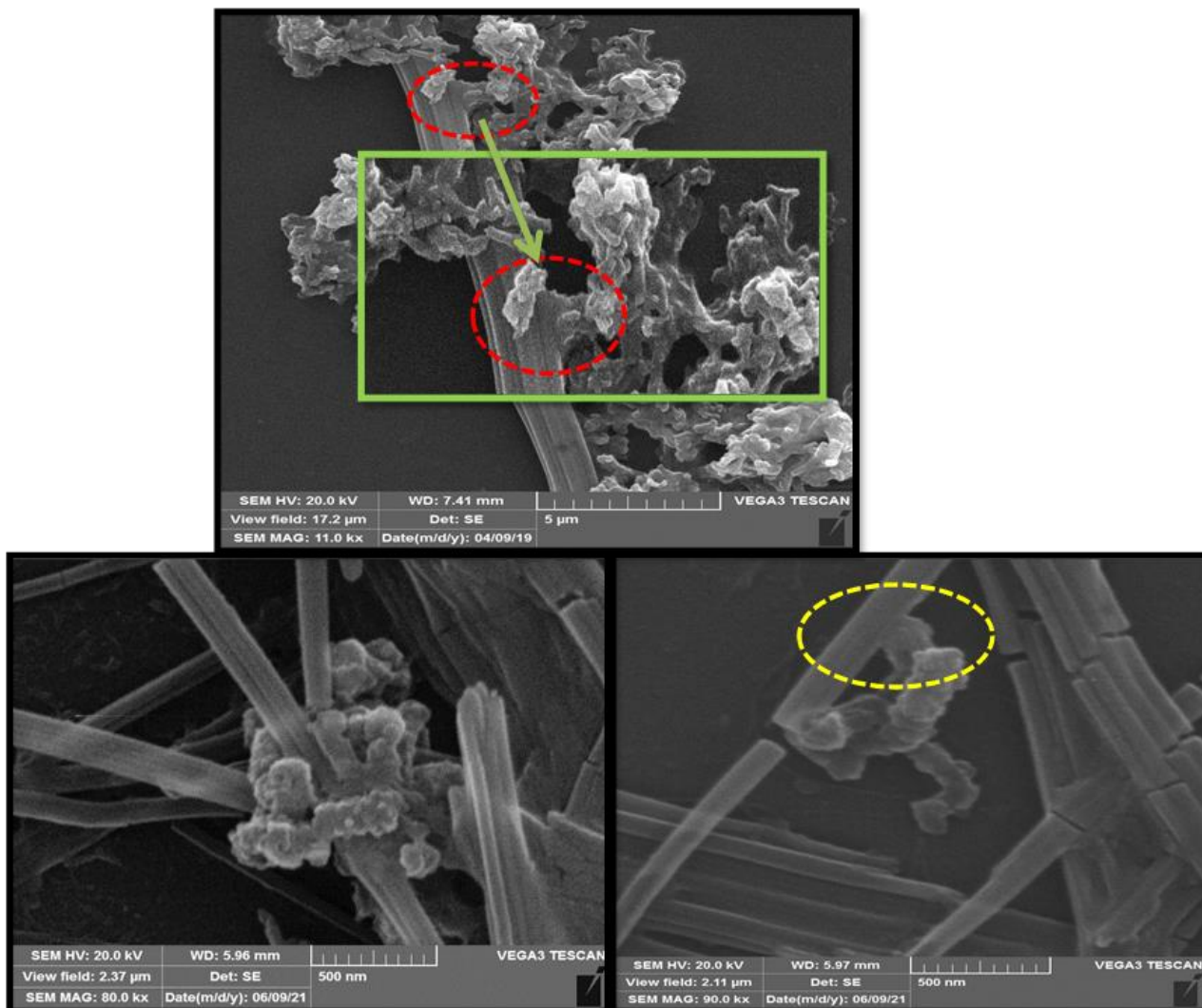


Figure S3. The SEM images of the interface between PANI and Cu(II)-L-aspartic acid nanofibers.

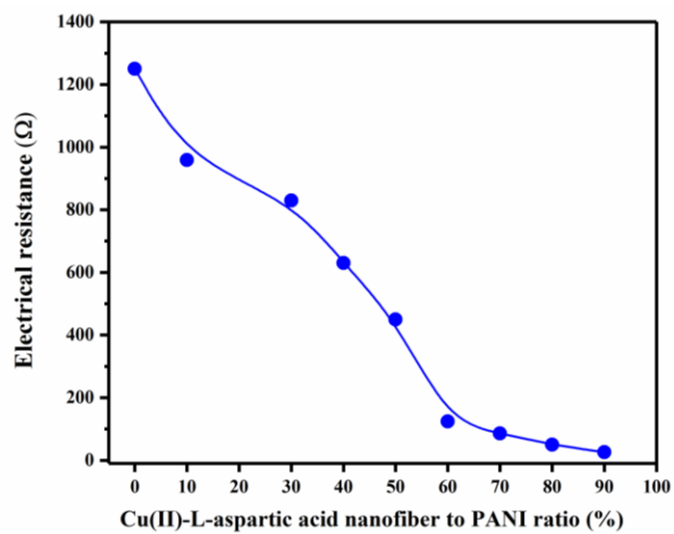


Figure S4. The electrical resistance of Cu(II)-L-aspartic acid nanofibers/PANI nanofibers sensor as a function of Cu(II)-L-aspartic acid nanofibers/PANI ratio.

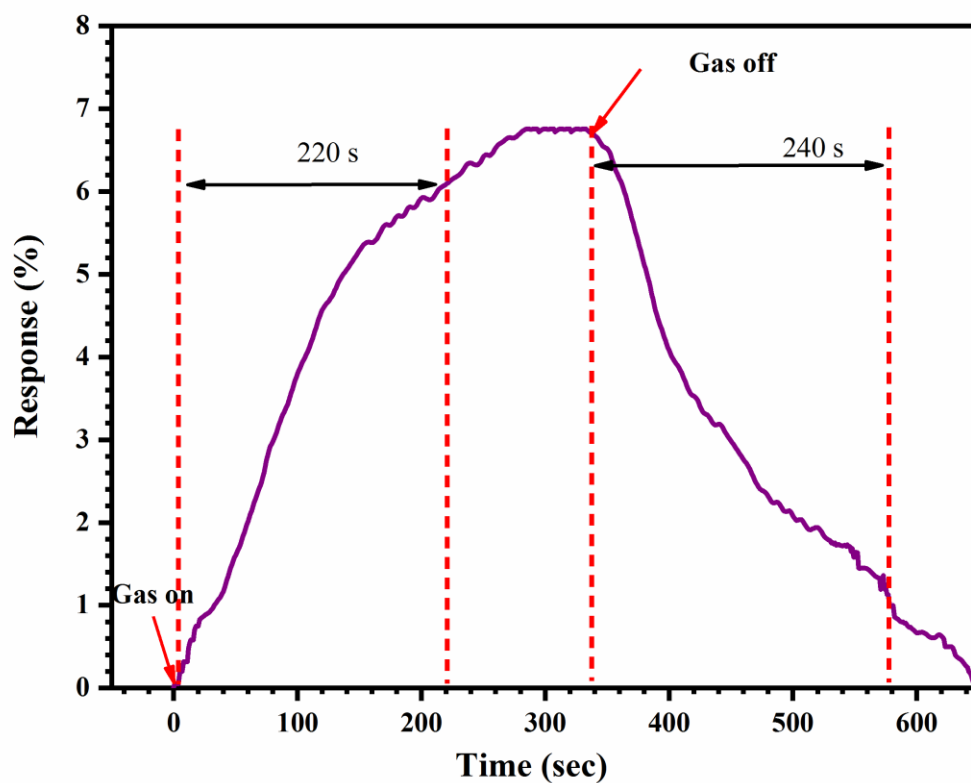


Figure S 5. The response and recovery times of the Cu(II)-L-aspartic acid nanofibers/PANI nanofibers sensor to 1000 ppm CO at room temperature.

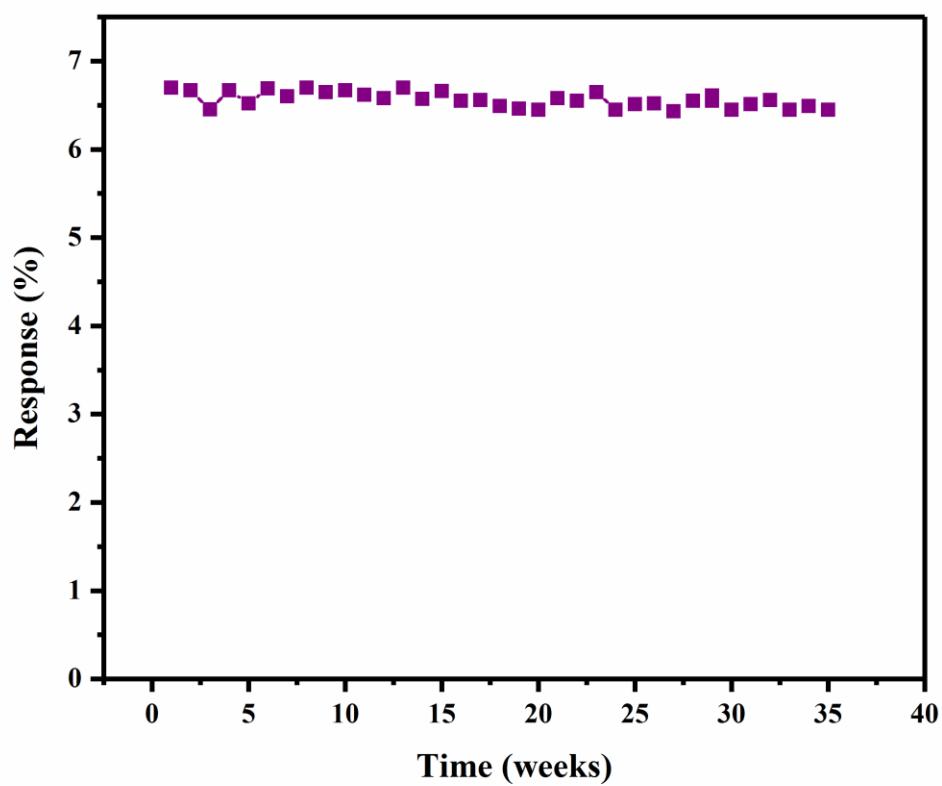


Figure S6. Plot of sensor stability to 1000 ppm of CO each weak over eight months.

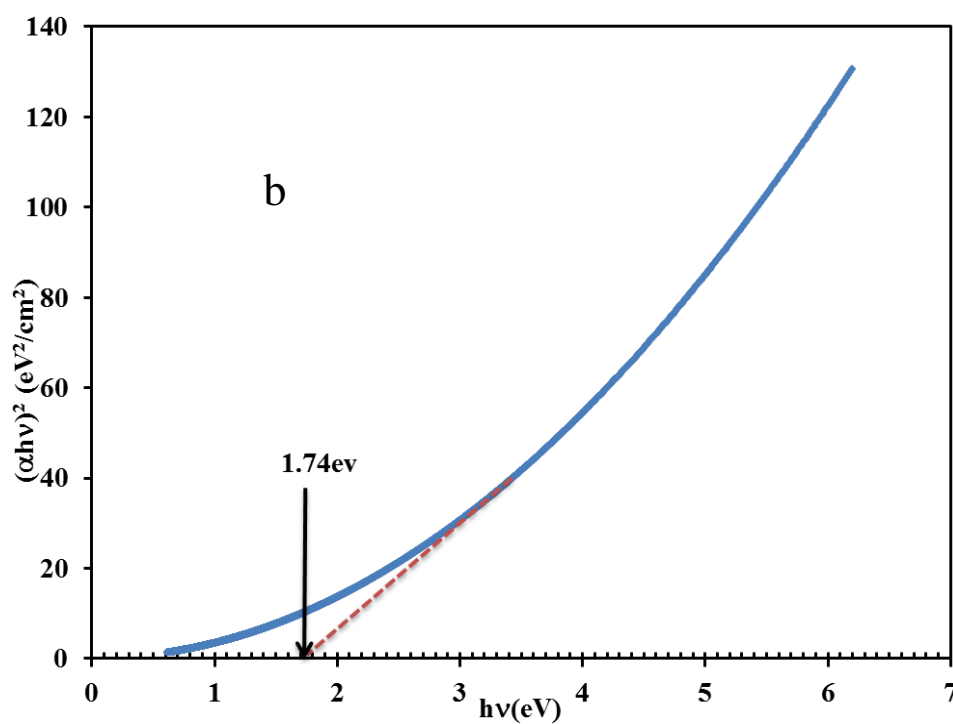
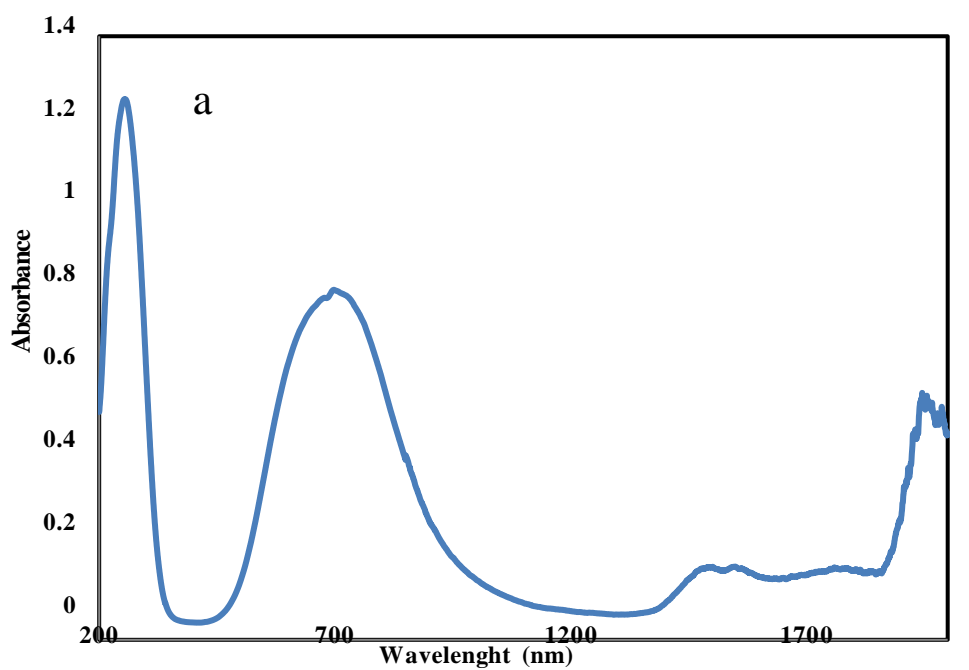


Figure S7. a) The solid UV-Vis absorption and b) Tauc plot of the Cu(II)-L-aspartic acid nanofibers derived from solid UV-Vis spectrum.

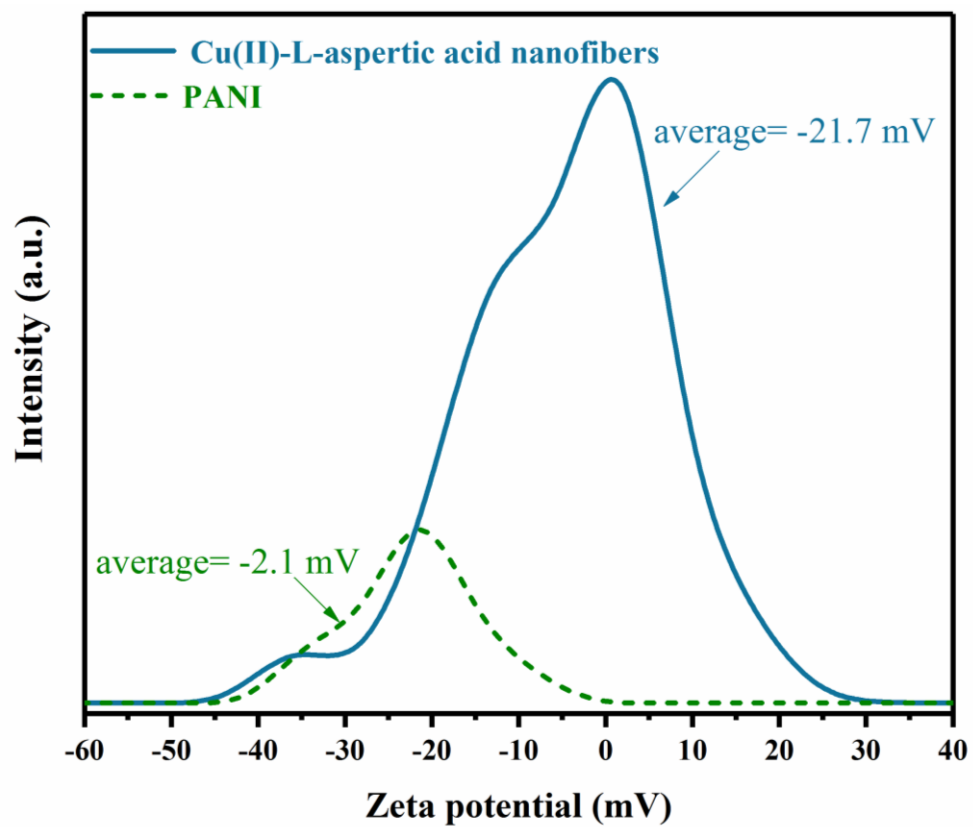


Figure S8. The average zeta potential for Cu(II)-L-aspartic acid nanofibers and PANI nanofibers.